

# **Beyond Breast Density:** Risk Measures for Breast Cancer in Multiple Imaging Modalities

Raymond J. Acciavatti, PhD\* • Su Hyun Lee, MD, PhD\* • Beatriu Reig, MD, MPH, • Linda Moy, MD • Emily F. Conant, MD • Despina Kontos, PhD\*\* • Woo Kyung Moon, MD, PhD\*\*

From the Department of Radiology, University of Pennsylvania, 3400 Spruce St, Philadelphia, PA 19104 (R.J.A., E.F.C., D.K.); Department of Radiology, Seoul National University Hospital, Seoul, South Korea (S.H.L., W.K.M.); and Department of Radiology, NYU Langone Health, New York, NY (B.R., L.M.). Received October 7, 2022; revision requested October 24; revision received November 23; accepted December 5. Address correspondence to R.J.A. (email: racci@pennmedicine.upenn.edu).

Supported by the Breast Cancer Alliance (2022 Young Investigator Grant); Burroughs Wellcome Fund (IRSA 1016451); National Research Foundation of Korea (NRF) funded by the Ministry of Science, ICT, and Future Planning (2022R1A2C1091282); U.S. Department of Defense Breast Cancer Research Program (W81XWH-18-1-0082); National Institutes of Health (NIH) National Cancer Institute (NCI) (5R01CA161749-09, 5R01CA207084-05, 1R37CA273959-01, and NCI P30 CA016520); NIH National Center for Advancing Translational Sciences (UL1TR001878); and, in part, by the Institute for Translational Medicine and Therapeutics (ITMAT) Transdisciplinary Program in Translational Medicine and Therapeutics at the University of Pennsylvania and the NCI/NIH at the New York University Grossman School of Medicine (P41EB017183).

\* R.J.A. and S.H.L. contributed equally to this work.

\*\* D.K. and W.K.M. are co-senior authors.

Conflicts of interest are listed at the end of this article.

Radiology 2023; 306(3):e222575 • https://doi.org/10.1148/radiol.222575 • Content code: BR

Breast density is an independent risk factor for breast cancer. In digital mammography and digital breast tomosynthesis, breast density is assessed visually using the four-category scale developed by the American College of Radiology Breast Imaging Reporting and Data System (5th edition as of November 2022). Epidemiologically based risk models, such as the Tyrer-Cuzick model (version 8), demonstrate superior modeling performance when mammographic density is incorporated. Beyond just density, a separate mammographic measure of breast cancer risk is parenchymal textural complexity. With advancements in radiomics and deep learning, mammographic textural patterns can be assessed quantitatively and incorporated into risk models. Other supplemental screening modalities, such as breast US and MRI, offer independent risk measures complementary to those derived from mammography. Breast US allows the two components of fibroglandular tissue (stromal and glandular) to be visualized separately in a manner that is not possible with mammography. A higher glandular component at screening breast US is associated with higher risk. With MRI, a higher background parenchymal enhancement of the fibroglandular tissue has also emerged as an imaging marker for risk assessment. Imaging markers observed at mammography, US, and MRI are powerful tools in refining breast cancer risk prediction, beyond mammographic density alone.

© RSNA, 2023

ndividuals with dense breasts are at higher risk for breast cancer, as well as cancer masking by dense breast tissue, than individuals at otherwise similar risk who have less dense breasts (1,2). Breast density refers to fibroglandular tissue, which has both "fibrous" (stromal) and glandular (lobular and ductal) components (3). Fibroglandular tissue appears dense (white) on both two-dimensional digital mammography (DM) and digital breast tomosynthesis (DBT) images; adipose tissue appears darker (4). Breast density tends to decrease with age, having children, and tamoxifen use (an estrogen blocker), but increases with lower body mass index and hormonal replacement therapy (5–9).

The prevalence of mammographically dense breasts is approximately 43% in women aged 40–74 years in the United States (10). In addition to notification of mammographic density (11), supplemental screening with whole-breast US or MRI can be considered in women with dense breasts due to the combination of masking of cancers by dense breast tissue and the increase in cancer risk with increasing breast density. These supplemental screening modalities offer higher sensitivity in women with dense breasts, but with the trade-off of increasing the number of false-positive findings (12,13).

Breast cancer most frequently arises from ductal and glandular elements of the breast. This article provides an

overview of imaging markers of these structures. In DM and DBT, risk is measured through the amount and textural complexity of dense fibroglandular tissue. Breast US offers the ability to visualize the two components of fibroglandular tissue separately (stromal and glandular) and, thus, measure risk in terms of the relative proportion of glandular to stromal tissue. Breast MRI quantifies the dynamic enhancement of normal breast parenchyma, also an independent imaging marker. Similar to MRI, increased background parenchymal enhancement (BPE) levels at contrast-enhanced mammography (14,15) and background parenchymal uptake at molecular breast imaging (16) may be an indication of breast cancer risk and, thus, is important to report. However, as of November 2022, contrast-enhanced mammography and molecular breast imaging are not widely used and, hence, they are not included in the current review.

# DM and DBT

## Mammographic Density

Early works in mammography assessed breast cancer risk with categorical measures, including the four patterns defined by Wolfe (17), the Tabár classification of five categories based on histopathologic-mammographic correlations (18), and the six categories of percent density

This copy is for personal use only. To order printed copies, contact reprints@rsna.org

#### **Abbreviations**

AUC = area under the receiver operating characteristic curve, BI-RADS = Breast Imaging Reporting and Data System, BPE = background parenchymal enhancement, DBT = digital breast tomosynthesis, DM = digital mammography, SM = synthetic mammography

#### Summary

Going beyond mammographic density, this article describes the range of imaging markers associated with breast cancer risk in digital mammography, digital breast tomosynthesis, whole-breast US, and MRI.

#### Essentials

- Breast density assessed with digital mammography or digital breast tomosynthesis is an independent risk factor for developing breast cancer and is included in several risk-assessment models.
- Beyond mammographic density, the spatial arrangement of fibroglandular tissue can be assessed with radiomic features and deep learning, identifying complex parenchymal patterns associated with higher risk.
- While both stromal and glandular components of fibroglandular tissue appear bright or "dense" on mammograms, breast US allows the two components to be visualized separately in a manner that is not possible with mammography; a higher glandular component at screening breast US is associated with higher risk for breast cancer.
- On breast MRI scans, higher background parenchymal enhancement of normal fibroglandular breast tissue is associated with a higher risk for breast cancer.

proposed by Boyd et al (19). To standardize clinical image interpretations, the American College of Radiology developed the Breast Imaging Reporting and Data System (BI-RADS) with four risk categories in DM and DBT based on breast density (Fig 1). The 4th edition (20) used percent density in assess-

ing risk. In the 5th edition (21), percent density was removed. Instead, the impact of breast density on obscuring or "masking" underlying cancer (degree of masking) is emphasized (Table 1). The classifications are as follows: (a) almost entirely fatty; (b) scattered areas of fibroglandular density; (c) heterogeneously dense, which may obscure detection of small masses; and (d) extremely dense, which lowers the sensitivity of mammography. An example of a breast that would be classified differently by the two editions is one with a high concentration of fibroglandular tissue in a single area (Fig 2) but less than 51% percent density. This breast would be classified as "category 2: scattered densities (approximately 25%-50% glandular)" according to the 4th edition. However, this breast would be categorized as "category C: heterogeneously dense, which may obscure detection of small masses" according to the 5th edition because the dense retroareolar tissue could obscure lesions.

BI-RADS risk assessment is prone to interreader variability (22). Attempts have been made to standardize BI-RADS risk assessment with deep learning (23). For example, Lehman et al (24) found that 90% of four-category classifications with DM using deep learning were accepted by the interpreting radiologist. Additionally, 94% of binary (dense vs nondense) classifications were accepted by the radiologist; among discordant classifications, 33% were downgraded from dense to nondense, whereas 67% were upgraded from nondense to dense. As noted in that work, results may have been impacted by changes in BI-RADS editions, with each edition offering a different perspective on breast cancer risk. The 4th edition emphasizes the role of percent density in breast cancer risk prediction, yet the 5th edition emphasizes the role of dense tissue in cancer masking (reducing sensitivity).

As an alternative to categorical measures of density, previous works have calculated area-based percent density (total dense

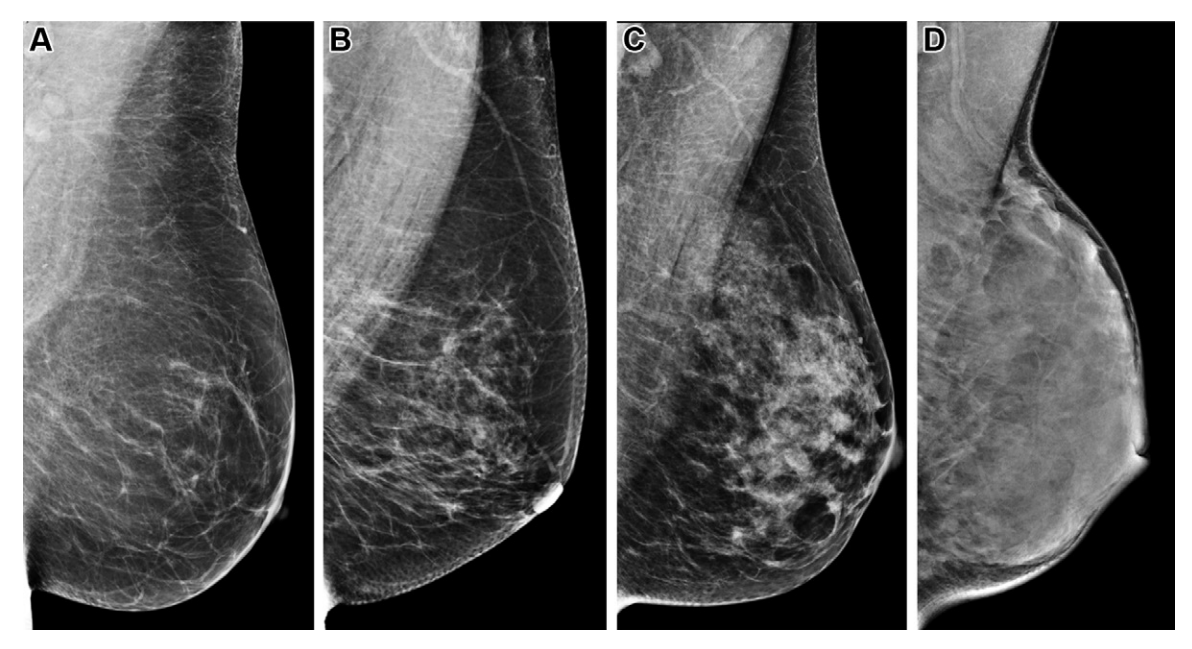


Figure 1: Mediolateral oblique digital mammograms illustrating the four categories of visually assessed breast density according to the 5th edition of the Breast Imaging Reporting and Data System show (A) breast that is almost entirely fatty; (B) breast with scattered areas of fibroglandular density; (C) breast that is heterogeneously dense, which may obscure detection of small masses; and (D) breast that is extremely dense, which lowers the sensitivity of mammography. Of note, with increasing higher density, there is a higher risk of breast cancer.

Edition and Category	Breast Tissue Characteristics
BI-RADS, 4th edition	
1	Almost entirely fatty (<25% glandular)
2	Scattered densities (approximately 25%–50% glandular)
3	Heterogeneously dense (approximately 51%–75% glandular)
4	Extremely dense (>75% glandular)
BI-RADS, 5th edition	
A	Almost entirely fatty
В	Scattered areas of fibroglandular densit
С	Heterogeneously dense, which may obscure detection of small masses
D	Extremely dense, which lowers the sensitivity of mammography

Note.—The four BI-RADS categories are based on the percent density (4th edition) and the degree of masking (5th edition). BI-RADS = Breast Imaging Reporting and Data System.

area relative to breast area). The reference standard software for this calculation is Cumulus (University of Toronto), which enables manual segmentation of dense tissue. Attempts have been made to automate the calculation with deep learning (25–27), and similarity to manual segmentation of dense tissue has been demonstrated, for example, with Dice coefficients of 63% in Kallenberg et al (25) and 76% in Li et al (26). As of November 2022, there are at least nine U.S. Food and Drug Administration—approved density assessment methods for DM, DBT, and synthetic mammography (SM) using artificial intelligence (28).

One application of area-based percent density is discriminating individuals at high risk from those at low risk. For example, Maghsoudi et al (27) used multiple research and commercial density assessment methods to distinguish cases that developed cancer an average of 4.7 years after a negative or benign DM examination from controls. Areas under the receiver operating characteristic curve (AUCs) ranged from 0.557 to 0.619, similar to other works (25,29,30) analyzing area-based percent density. An AUC of 0.70 or greater is considered acceptable for predictive modeling (31).

Breast density can also be assessed three-dimensionally by total dense volume (sum total of fibroglandular pixel volumes) and volumetric percent density (total dense volume relative to breast volume), for example, by using Quantra (Hologic) and Volpara (Volpara Health). To illustrate differences between these measures, four breasts with variations in total dense volume yet effectively equivalent volumetric percent density (approximately 25%) are shown (Fig 3). Brandt et al (32) found that volumetric percent density at DM offered stronger association with breast cancer risk than total dense volume.

# Augmenting Epidemiologically Based Models with Breast Density

Various works showed that augmenting epidemiologically based models with breast density improves AUC (33–35). Brentnall



**Figure 2:** Mediolateral oblique screening digital mammogram in a 56-year-old woman shows dense tissue in the anterior subareolar area of the breast (arrow). If assigned a Breast Imaging Reporting and Data System (BI-RADS) breast density based on the 4th edition, the percent density in the breast would be less than 51% and, therefore, would be considered category 2 or "scattered fibroglandular densities." However, if classified according to the 5th Edition of BI-RADS for density, the dense tissue in the anterior breast could "mask" or obscure a lesion, causing a reduction in detection sensitivity. Based on the density definitions in the 5th Edition, this breast would be considered "heterogeneously dense, which may obscure detection of small masses."

et al (35) augmented the Gail and Tyrer-Cuzick models with radiologist visual assessment of area-based percent density, improving the AUCs from 0.55 to 0.59 and from 0.57 to 0.61, respectively, for 10-year risk assessment.

As of November 2022, at least three risk-assessment models incorporate mammographic density (Table 2). For example, in the Tyrer-Cuzick model (version 8), mammographic density is typically measured in terms of volumetric percent density or BI-RADS density, as Brentnall et al concluded that total dense volume is a weaker predictor of risk than these two density measures (36). Adding breast density to the Tyrer-Cuzick model improved the accuracy of risk stratification for both women at high-risk (>8%, 10-year risk) and those at low-risk (<2%, 10-year risk). The percentage of patients considered high risk increased from 4.8% (without density) to 7.1% (BI-RADS density) and 6.8% (volumetric percent density).

#### Assessing Breast Texture with Radiomic Features

Breast parenchymal complexity quantifying the spatial arrangement of fibroglandular tissue is a separate measure of breast cancer risk. Parenchymal complexity can be assessed with

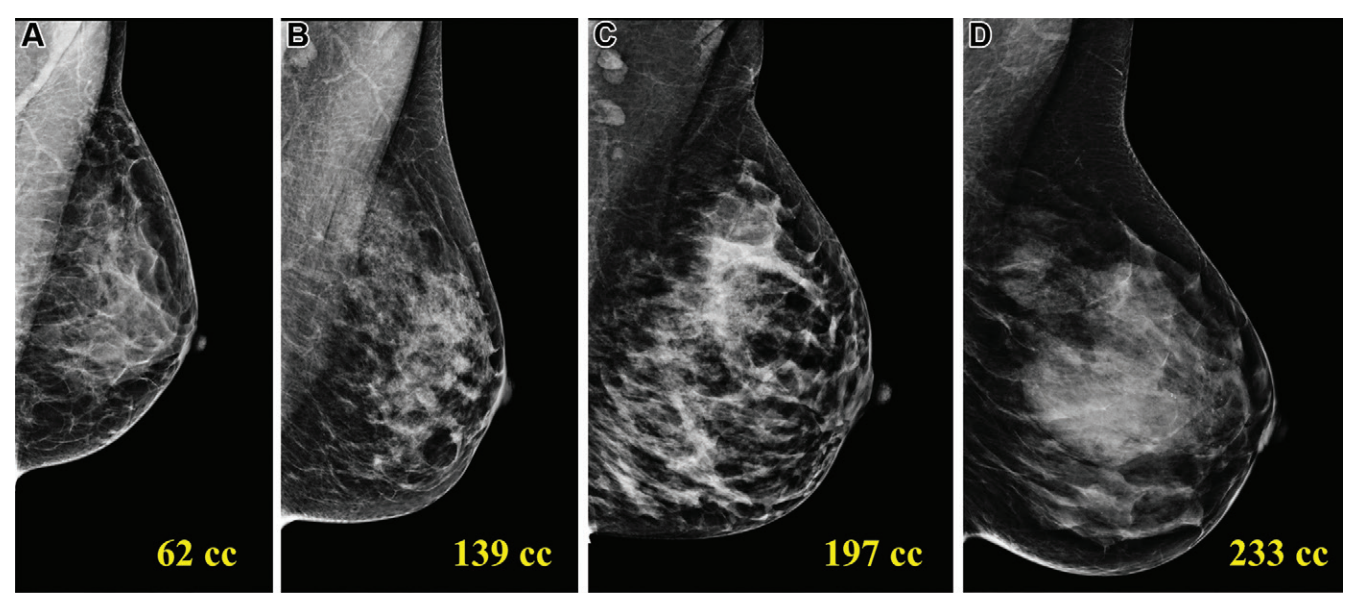


Figure 3: Mediolateral oblique digital mammograms in four different women show effectively equivalent volumetric percent density (approximately 25%) but broad variation in the total dense volumes, which range from 62 mL to 233 mL. Volume-based density measures include the total dense volume (sum total of all fibroglandular pixel volumes) and volumetric percent density.

Model	Input Variables	Output	Clinical Use
Tyrer-Cuzick (or IBIS model), version 8	Demographic and reproductive risk factors, first- and second-degree family history of breast and ovarian cancer, mammographic density (BI-RADS, Volpara, and/or visual analog scale), biopsy-confirmed benign breast disease, and breast cancer susceptibility genes (BRCA1 or BRCA2)	10-year and lifetime (to 85 years of age) risk of developing breast cancer	Risk assessment for MRI screening (20% lifetime risk as threshold)
Breast Cancer Surveillance Consortium (BCSC), version 2	Age, race and ethnicity, first-degree family history of breast cancer, mammographic density (BI-RADS), and biopsy-confirmed benign breast disease	5-year and 10-year risk of developing invasive breast cancer	Risk assessment for use of chemoprevention (1.67% 5-year risk as threshold)
Breast and Ovarian Analysis of Disease Incidence and Carrier Estimation Algorithm (BOADICEA), version 6	Demographic, lifestyle, and reproductive risk factors, first- and second-degree family history of breast and ovarian cancer, mammographic density (BI-RADS), polygenic risk scores, and breast and/or ovarian cancer susceptibility genes (BRCA1, BRCA2, PALB2, ATM, CHEK2, BARD1, RAD51C, and RAD51D)	5-year, 10-year, and lifetime (to 80 years of age) risk of developing breast and ovarian cancer; variant carrier probabilities	Risk assessment for genetic testing (10% likelihood of carrying a <i>BRCA1</i> or <i>BRCA2</i> variant as threshold)

high-throughput extraction of radiomic features (37), which can be visualized in DM with heat maps of the breast area; skewness (a gray-scale feature) and entropy (a co-occurrence feature) are examples (Fig 4) (38). Examples of breasts varying in terms of both density and complexity are illustrated in Figure 5 (39).

In some works (40,41), a single region of interest is used in radiomic feature extraction. Alternatively, multiple regions of interest capture heterogeneities in breast texture. Sun et al (42) partitioned the breast into five subregions varying from the densest region to the whole breast. In assessing near-term risk (the risk

of cancer at the next DM examination), the AUC in case-control classification was higher when extracting radiomic features from different subregions as opposed to the whole breast. Zheng et al (38) created a lattice of windows for radiomic feature extraction in DM, with cases defined by the contralateral image of a cancerpositive mammogram. That work found case-control classification to be optimized with a 6.3 mm window size (the smallest considered); that is, AUCs of 0.59 (area-based percent density), 0.85 (radiomics), and 0.86 (radiomics plus area-based percent density).

Another application of radiomics is discriminating *BRCA1* and *BRCA2* variant carriers from controls (43–45). Clinically,

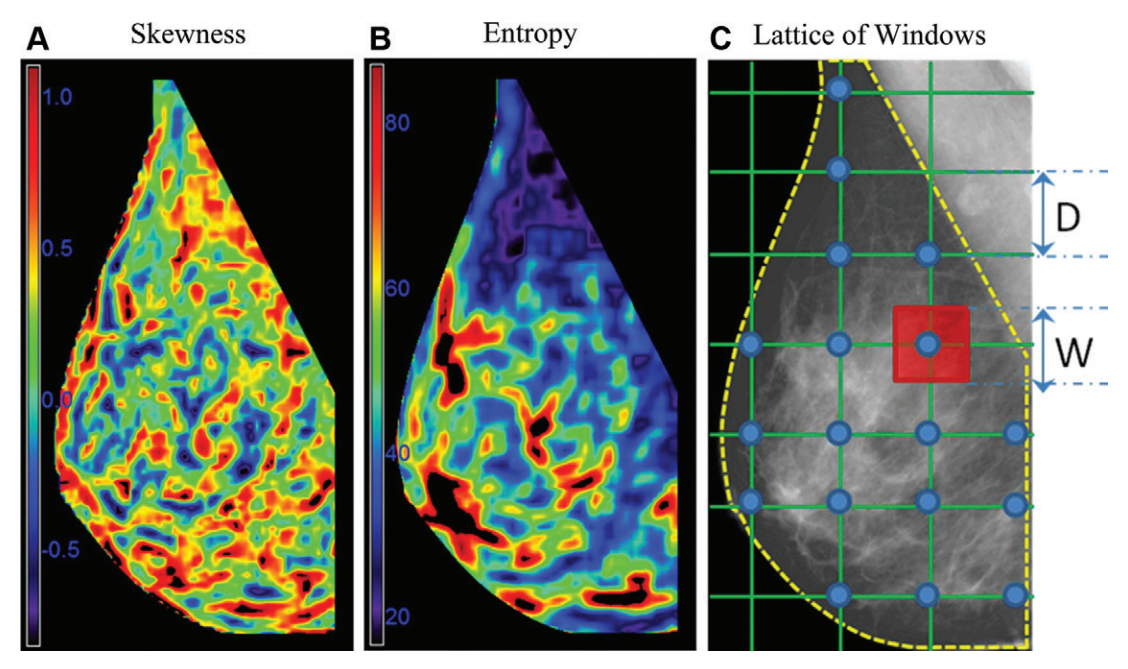


Figure 4: (A, B) Digital mammographic heat maps show radiomic feature calculations in the breast area; for example, skewness (A) (a gray-scale feature) and entropy (B) (a co-occurrence feature). (C) To capture heterogeneities in breast texture in the breast area (dashed yellow line), radiomic features can be calculated in multiple windows whereby each window (example in red, with the length of each side defined as W) is centered on a lattice point (blue circle) and green lines define the lattice grid, with the spacing between lattice points defined as D. (Reprinted, with permission, from reference 38.)

this may prove important if a patient's genetic history is unknown. For example, Li et al (45) showed that radiomic features (AUC, 0.81) performed better than area-based percent density (AUC, 0.53) for discriminating *BRCA1* and *BRCA2* variant carriers from controls.

# Deep Learning in Breast Cancer Risk Assessment

Recent advances in deep learning have allowed the computer to "learn" the features associated with breast cancer risk (23). Although handcrafted radiomic features could potentially be more interpretable, the advantage of deep learning is that features predictive of risk do not need to be known a priori.

Various works (46–48) have shown that deep learning models are more predictive of risk than mammographic density alone; for example, Arefan et al (46) analyzed cancer cases and controls using negative or benign DM images from at least 1 year prior. In that study, the deep learning model with the highest AUC (0.73) performed better than area-based percent density (AUC, 0.54). Ha et al (48) used a convolutional neural network-based pixelwise risk model to identify women at high-risk by analyzing negative mammograms from at least 2 years prior to cancer (with controls having at least a 2-year follow-up with negative findings). In pixel-wise heat maps, areas in red have features that overlap with patients who developed cancer, as opposed to normal areas in blue (Fig 6). Heat maps with substantially more red areas allow the patient at higher risk to be identified among two heterogeneously dense breasts (Fig 6A, 6B), as well as among breasts with scattered areas of fibroglandular density (Fig 6C, 6D), illustrating how risk is predicted in a manner separate from mammographic density.

Previous works have investigated deep learning to refine risk models in clinical use. For example, for 5-year risk assessment, Yala et al (49) evaluated the AUCs of a risk factor–based logistic regression model using traditional risk factors (AUC, 0.67), an image-only deep learning model for DM (AUC, 0.68), and a hybrid deep learning model combining traditional risk factors and DM images (AUC, 0.70). The hybrid deep learning model achieved a statistically significant gain in AUC over the Tyrer-Cuzick version 8 model (AUC, 0.62). Additionally, AUCs obtained with the Tyrer-Cuzick version 8 model differed by race and ethnicity (eg, 0.45 and 0.62 for African American and White women, respectively), yet AUCs obtained with the hybrid deep learning model were insensitive to race and ethnicity (0.71).

In a subsequent study, Yala et al (50) developed Mirai, a mammography-based deep learning model, to assess 1- to 5-year risk at DM. In a test set consisting of patients who developed cancer within 5 years, 41.5% of patients were successfully identified as high risk with Mirai as opposed to 36.1% with the hybrid deep learning model and 22.9% with the Tyrer-Cuzick version 8 model, illustrating how deep learning improves risk stratification over the Tyrer-Cuzick version 8 model.

# **Digital Breast Tomosynthesis**

As of November 2022, DBT has become widespread for mammography screening (51,52). DBT uses a reconstruction in combination with a two-dimensional image, obtained either with DM or SM (53,54). Previous works compared DM, DBT, and SM in terms of density assessments. Tice et al (55) found no difference in BI-RADS density classifications at DM and DBT in data from 2010 to 2017 (under the 4th and 5th editions of BI-RADS), and no difference in the strength of the association between mammographic density and invasive breast cancer. Haider et al (56) found that SM did not significantly change binary (dense vs nondense)

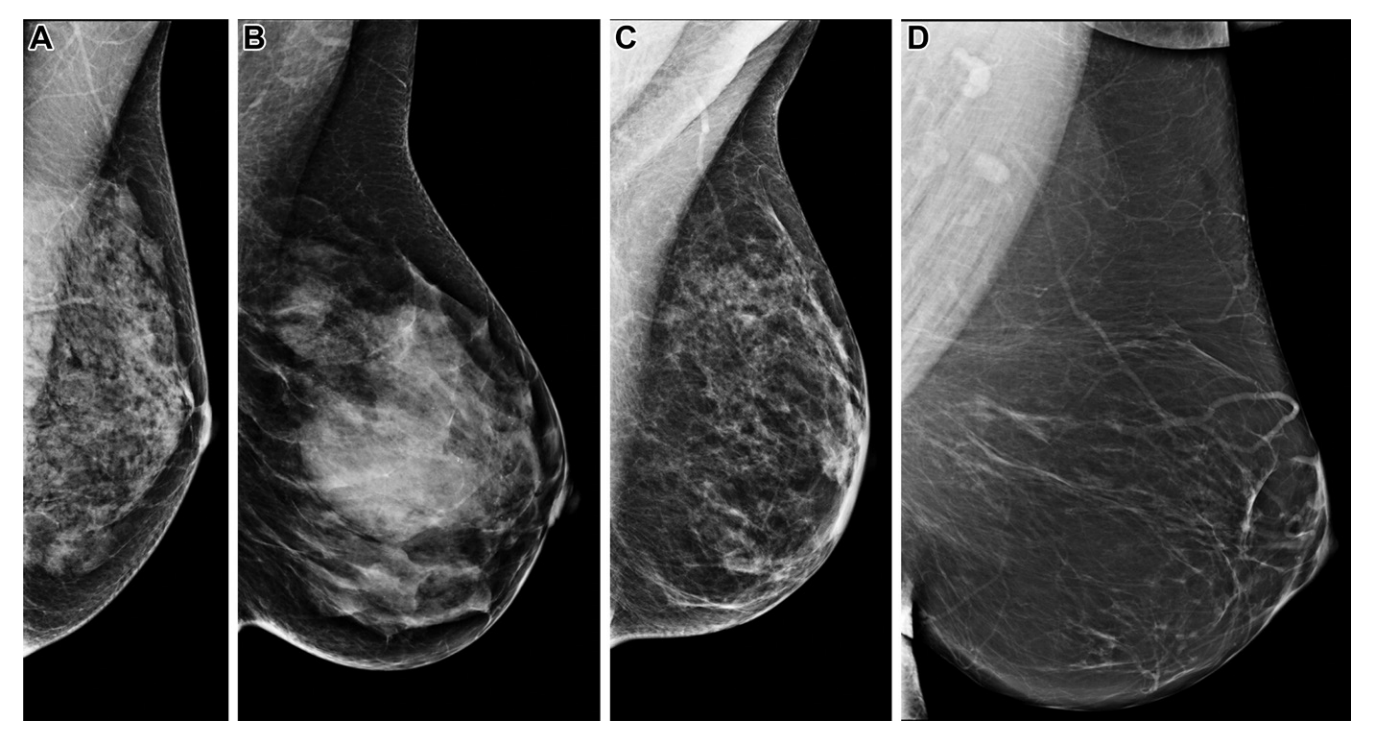


Figure 5: Mediolateral oblique digital mammograms with negative findings at screening in women with (A) high density and high complexity, (B) high density and low complexity, (C) low density and high complexity, and (D) low density and low complexity. Breast density is associated with higher risk for developing breast cancer. In addition, breasts with more complex parenchymal patterns are at higher risk for breast cancer. These parenchymal patterns were assessed with handcrafted radiomic features to develop an overall complexity score. (Reprinted, with permission, from reference 39.)

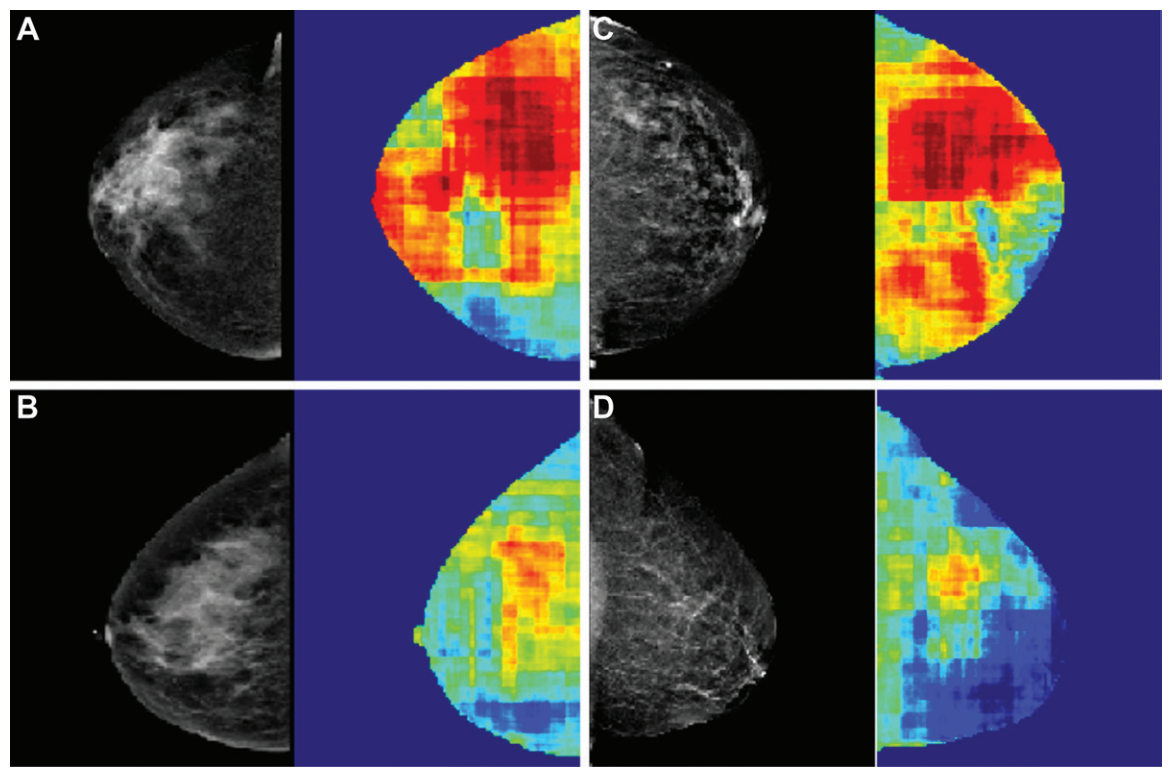


Figure 6: (A, B) Mammograms (left) of heterogeneously dense breasts are analyzed in terms of a convolutional neural network-based pixel-wise risk model (right), which identifies the breast at higher risk for cancer (A) by having more substantial areas in red, corresponding to features that overlap with patients who developed breast cancer, as opposed to normal (blue) areas. (C, D) Similarly, among two breasts with scattered areas of fibroglandular density at mammography (left), the breast at higher risk for cancer (C) is identified by having more substantial red areas (right). (Reprinted, with permission, from reference 48.)

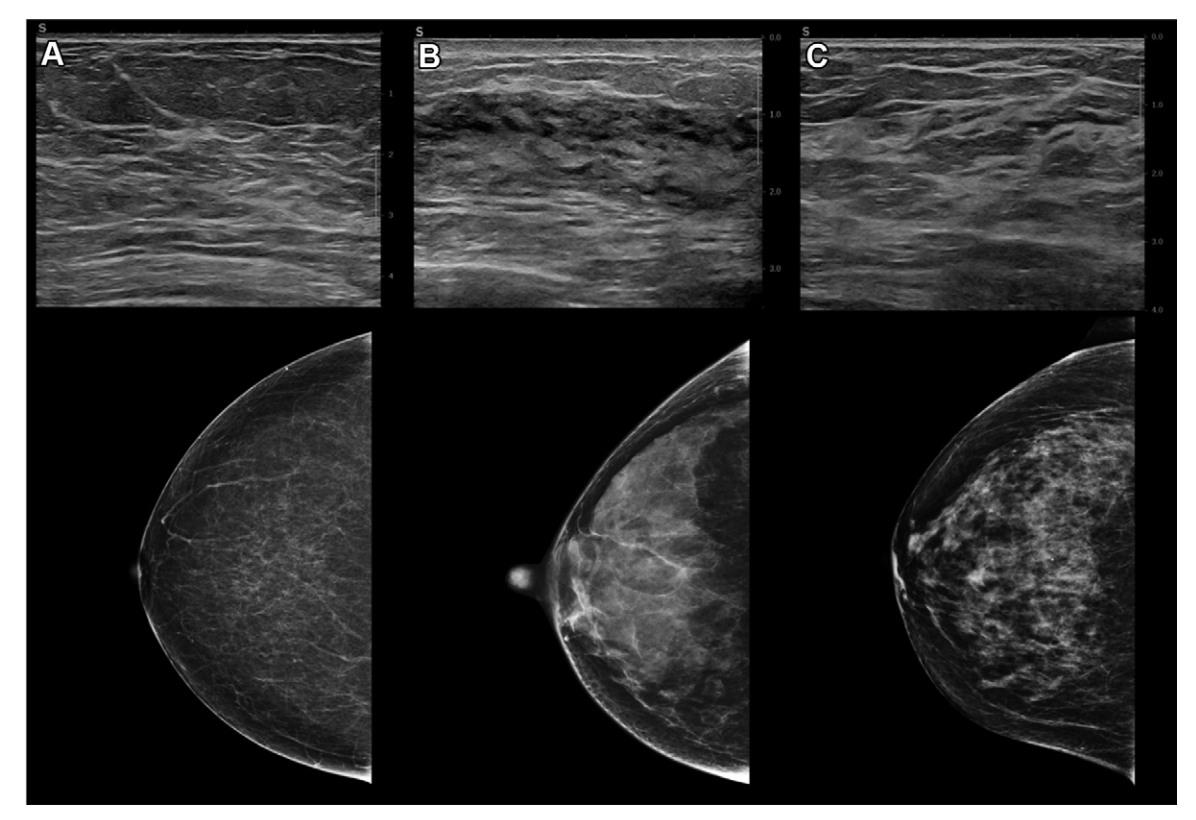


Figure 7: Top: Classification of tissue composition at breast US according to the Breast Imaging Reporting and Data System, 5th edition. Representative US images show (A) homogeneous background echotexture (fat), (B) homogeneous background echotexture (fibroglandular), and (C) heterogeneous background echotexture. Bottom: Corresponding craniocaudal mammograms show (A) almost entirely fat, (B) extremely dense, and (C) heterogeneously dense or scattered fibroglandular tissue at mammography.

classifications compared with DM. Other works, however, found that use of DBT with SM downgraded BI-RADS density classifications (57–59); Aujero et al (58) and Zuckerman et al (59) suggested that this may be related to perceptual adaptation to SM.

Lotter et al (60) applied deep learning to detect cancers in DBT based on the use of a maximum suspicion projection. Risk modeling in DBT is still an open area of research. Given that deep learning is already computationally intensive in DM, future applications in DBT are expected to be even more computationally demanding. At a typical DBT examination, 300 images may be produced while only four images are produced at DM. Deep learning in DBT is also challenging due to the anisotropic voxels (differing sizes in three directions) and variations in the compressed breast thickness. Early studies suggested improved performance in DBT risk prediction compared with DM data alone (60,61). Eriksson et al (61,62) showed that combining deep learning features (density, calcifications, masses) with familial, demographic, lifestyle, and polygenic risk scores achieved a higher AUC for a 2-year risk model (DM = 0.73, DBT = 0.83) than the Tyrer-Cuzick version 8 model (AUC, 0.62).

#### **Breast US**

# Tissue Composition at Breast US: BI-RADS Classification

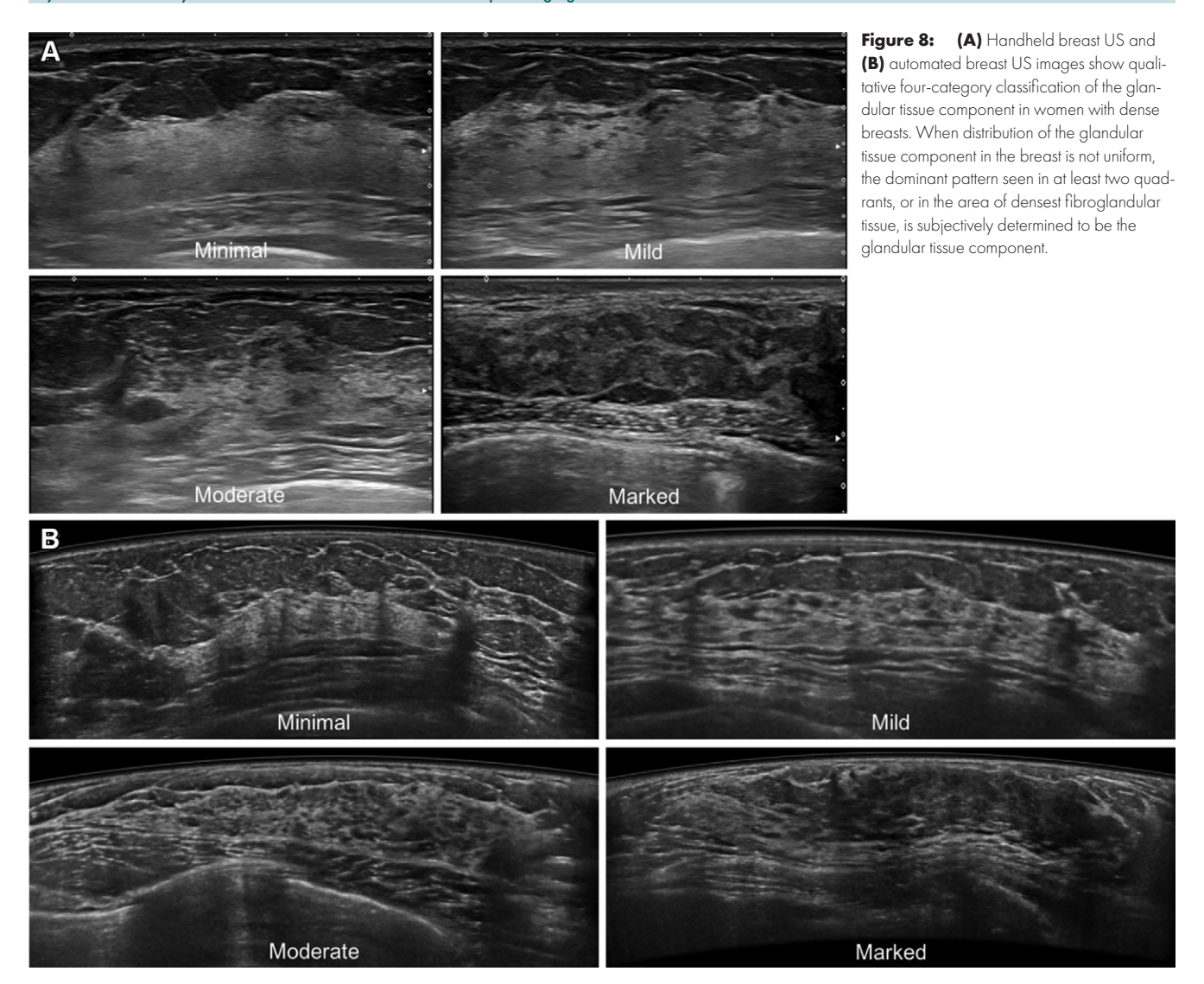
Tissue composition at breast US is classified as homogeneous background echotexture (fat), homogeneous background

echotexture (fibroglandular), and heterogeneous background echotexture according to the BI-RADS, 5th edition (63). These three categories correspond loosely to the four density descriptors of mammography (Fig 7). Dense breasts on mammograms usually fall within the homogeneous background echotexture (fibroglandular category), defined as a thick layer of fibroglandular tissue beneath the subcutaneous fat layer, irrespective of the internal echogenicity patterns within the fibroglandular tissue.

In several studies on US assessments of mammographic parenchymal patterns or breast density, a significant correlation between mammographic and US assessments was found (64–66). In a prospective study by Kim et al (67), assessments of breast density using real-time US was in exact agreement with 86% of mammograms when BI-RADS density categories were dichotomized into fatty (almost entirely fatty and scattered areas of fibroglandular density) and dense (heterogeneously dense and extremely dense).

#### Internal Echogenicity Patterns of Fibroglandular Tissue

The sonographic appearance of fibroglandular tissue may vary between individuals and over time in the same individual (68). Several studies have proposed methods for classifying internal echogenicity patterns within the fibroglandular tissue. Hou et al (69) classified sonographic parenchymal patterns into four types (heterogeneous, ductal, mixed, and fibrous) based on the different compositions of ducts, fibroglandular tissue, and fat



lobules. Lee et al (70) evaluated the proportions of isoechoic or hypoechoic areas representing glandular tissue relative to hyperechoic areas representing fibrous stroma in the fibroglandular tissue. The authors classified the amount of glandular tissue component in the fibroglandular tissue as minimal, mild, moderate, or marked (Fig 8). The glandular tissue component was visually estimated after scanning the entire breast. Sonographic glandular tissue component classification can be estimated more easily in the large field of views of automated breast US (71,72). The differences in the evaluation of the glandular tissue component and BI-RADS tissue composition are summarized in Table 3.

#### Internal Echogenicity Patterns and Breast Cancer Risk

The association of internal echogenicity patterns of fibroglandular tissue with breast cancer risk is explained by the fact that breast US can be used to distinguish between glandular and stromal tissues in the fibroglandular tissue on the basis of their echogenicity in a manner that is not possible with mammography. Breasts that appear similarly dense at mammography may show a wide spectrum of patterns at breast US and histologic assess-

ment, with predominantly hyperechoic fibrous tissue at one extreme and abundant isoechoic or hypoechoic glandular tissue at the other (Fig 9). The breast lobule or terminal duct lobular unit is known to be the primary anatomic source of breast cancer, and the progressive degrees of lobular involution are associated with a reduced risk of developing breast cancer (73). Women with dense breasts on mammograms have varying degrees of lobular involution (74) and, therefore, may have different breast cancer risk, which could be stratified by sonographic glandular tissue component assessment. A previous study in 233 women showed that a higher glandular tissue component at breast US is associated with less degree of lobular involution (70).

A recent retrospective study that included 541 women with cytopathologic confirmation of cancer and 849 age-matched women without cytopathologic confirmation of breast cancer evaluated four types of sonographic parenchymal patterns (75). The authors showed that the heterogeneous type (odds ratio, 3.97; P < .001) and fibrous type (odds ratio, 2.70; P < .001) were associated with breast cancer. Another recent retrospective cohort study evaluated the association between the glandular tissue component on breast US images and future breast cancer risk

Component	Tissue Composition (BI-RADS, 5th edition)	Glandular Tissue Component
Definition	Balance between the fibroglandular tissue and fat, similar to mammographic density	Proportion of the glandular tissue in the fibroglandular tissue
Classification	Homogeneous background echotexture (fat), homogeneous background echotexture (fibroglandular) or heterogeneous background echotexture	Four category (minimal, mild, moderate, , marked) or dichotomous (low, high)
Observer variability	Kappa value of 0.30 (kappa of 0.30 for homogeneous, 0.19 for focally heterogeneous, and 0.41 for diffusely heterogeneous echotexture) (112)	Average kappa, 0.41 for the four-category classification and 0.52 for the dichotomous classification (70)
Effect on US sensitivity and specificity	Detection of small and subtle lesions may be confounded by heterogeneous background echotexture	A high glandular tissue component was associated with a higher abnormal interpretation rate than a low glandular tissue component (20.1% vs 8.5%; <i>P</i> < .001) at supplemental screening breast US (113)
Association with breast cancer risk	Unknown as of November 2022	Compared with a minimal or mild glandular tissue component, a moderate or marked glandular tissue component was associated with a higher cancer risk (hazard ratio, 1.5; $P = .03$ ) after adjusting for age and breast density (70)

(70). Among the 8483 women with mammographically determined dense breasts who underwent supplemental US screening, 137 (1.6%) developed breast cancer during a median follow-up time of 5.3 years. The incidence of breast cancer in women with a high glandular component was significantly higher than in women with a low glandular component (P = .01). In multivariable analysis, the baseline glandular tissue component was the only factor associated with breast cancer risk (hazard ratio, 1.5; P = .03) after adjusting for other risk factors, including age, menopausal status, history of benign breast biopsy, family history of breast cancer, and breast density.

# Future Directions for Breast Cancer Risk Assessment Using Breast US

Internal echogenicity patterns of the fibroglandular tissue at breast US have the potential for breast cancer risk assessment. However, standardization of evaluation methods for this new imaging marker is important prior to clinical implementation. Further studies on quantification and deep learning models will enhance robust and reproducible assessment. In addition, prospective multicenter studies are needed to validate the association between the glandular tissue component and breast cancer risk. A prospective multinational cohort study to validate the association of sonographic glandular tissue component and breast cancer risk has been published (ClinicalTrials.gov registration no. NCT05460975).

# **Breast MRI**

#### **MRI** Overview

Breast MRI is the most sensitive imaging modality for detection of breast cancer, including ductal carcinoma in situ and invasive cancers (76). Breast MRI can also be used to evaluate features of normal breast tissue that can inform breast cancer risk assessment. The amount of fibroglandular tissue assessed at MRI follows the same four categories as the BI-RADS 5th edition for mammographic density: almost entirely fat, scattered fibroglandular tissue, heterogeneous fibroglandular tissue, and extreme fibroglandular tissue (77). Normal fibroglandular tissue enhances after the administration of gadolinium-based contrast material and is known as BPE. BPE levels are qualitatively assessed as minimal, mild, moderate, or marked using the BI-RADS lexicon (Fig 10) or may be quantitively assessed using software. BPE is an independent risk factor for the development of breast cancer, separate from mammographic density (78).

#### **Biologic Underpinnings**

The biologic underpinnings of BPE have not been fully elucidated. Evidence suggests that BPE is related to endogenous and exogenous hormone levels; BPE varies with the phase of the menstrual cycle (79,80) and menopausal status (81), and BPE is reduced in women taking aromatase inhibitors and selective estrogen receptor modulators (82,83). Therefore, BPE likely partially reflects the effect of hormonal stimulation on the glandular components of the breast, which itself is associated with a higher risk of breast cancer. It is theorized that a second additional component of BPE is likely to be proliferative tissue changes, such as atypia, which are also associated with a higher cancer risk (84). Whether the cause of BPE is hormonal or due to proliferative change could be determined on the basis of whether BPE decreases after the cessation of hormonal stimulation, such as after menopause or after risk-reducing salpingo-oophorectomy. In BRCA1 and BRCA2 variant carriers who underwent risk-reducing salpingo-oophorectomy (85,86), a lack of BPE suppression would suggest that the underlying cause of BPE is proliferative change, including atypia, rather than hormonal stimulation. However, as discussed hereafter, studies show conflicting results as to whether these patients remain at higher risk for breast cancer. Additionally, several studies have found similar odds ratios for BPE and risk in premenopausal and postmenopausal groups (87,88), suggesting that endogenous estrogen does not affect the levels of BPE that reflect risk. It is possible that BPE is due to different processes in premenopausal and postmenopausal women, and in those with high and average risk. The biologic underpinnings of BPE and the relationship of BPE-associated risk to menopausal status for women at both average and high risk for breast cancer requires additional study.

# BPE and Breast Cancer Risk

The amount of fibroglandular tissue is reflected in mammographic density and is associated with breast cancer risk. BPE is independent of mammographic density and instead is associated with higher tissue microvascular density, expression of vascular endothelial

growth factor (89), and higher metabolic activity (79,87), representing an independent measure of tissue at risk. Women with dense breasts but minimal BPE do not have elevated breast cancer risk (87), suggesting that BPE may be a more accurate predictor of risk than density alone.

The association between BPE and breast cancer risk was first described in a case-control study of women at high risk, finding that women with moderate or marked BPE had a 6.7 times higher odds ratio of developing cancer than women with minimal or mild BPE (78). Additional single-institution, case-control, retrospective cohort, and cross-sectional studies that used BPE in breast MRI for risk assessment have yielded similar findings with odds ratios ranging from 1.45 to 14.5 depending on the patient population and BPE threshold (Table 4).

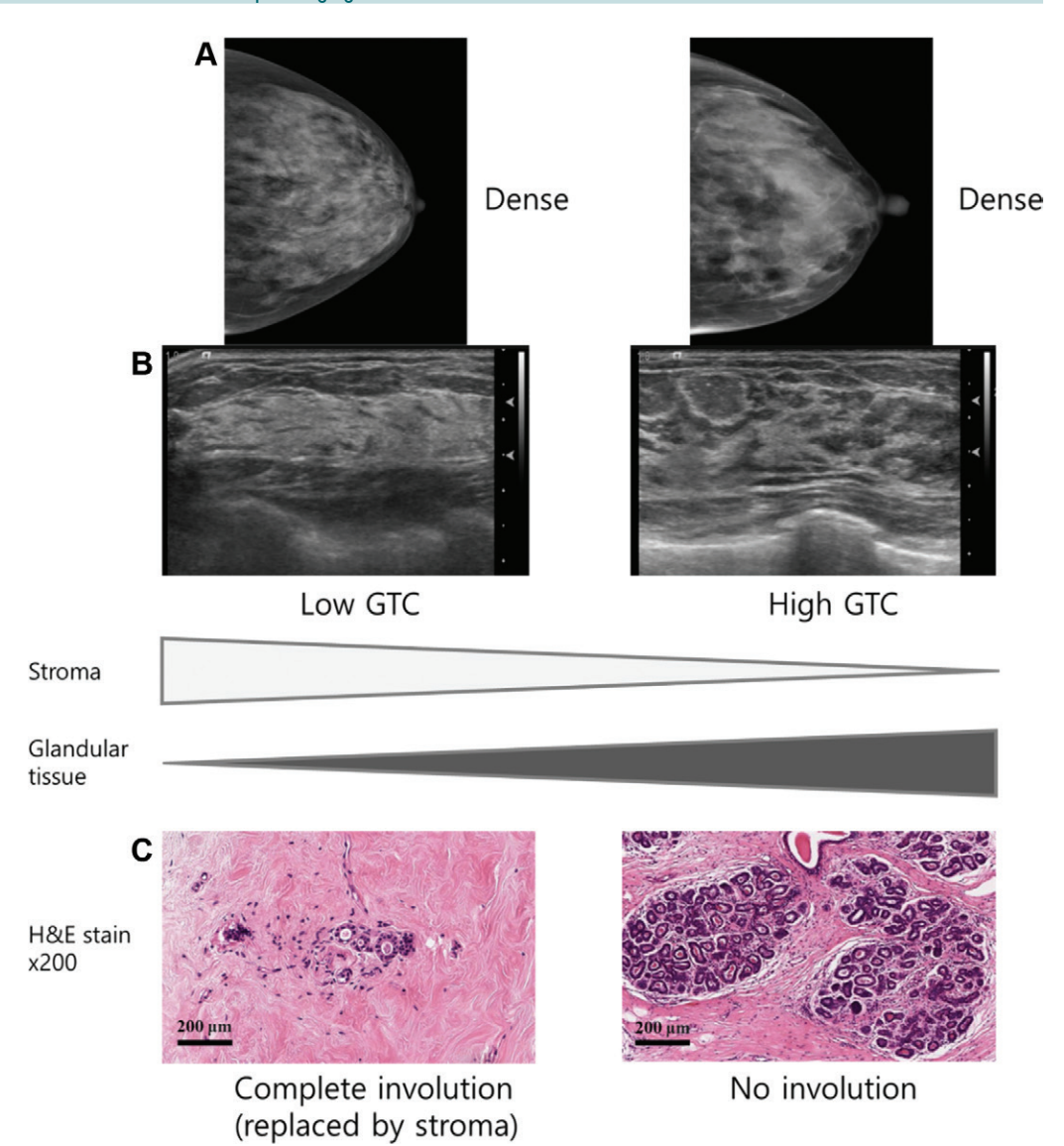


Figure 9: Spectrum of sonographic and histologic appearance of dense breasts at mammography. (A) Craniocaudal mammograms show extremely dense fibroglandular tissue in both cases. (B) Breast US images show predominately hyperechoic fibrous tissue at one end (left) and abundant isoechoic or hypoechoic glandular tissue at the other end (right) of the spectrum. (C) Histologic images (hematoxylin-eosin [H&E] stain; original magnification, x200) show the breast lobules are involuted and replaced by fibrous stroma in the former case (left), whereas the lobular involution is minimal and the size and number of acini per lobule is large in the latter case (right). GTC = glandular tissue component. (Reprinted, with permission, from reference 70.)

Since these early studies, meta-analyses (90,91) have corroborated the findings regardless of study design, timing of BPE measurement, and method of BPE assessment. Thompson et al (90) evaluated 18 studies for a total of 1910 women with breast cancer and 2541 control participants. In women at high risk, they found that at least mild BPE was associated with breast cancer with a 2.1 odds ratio. This odds ratio was reproduced across multiple studies when those with unmatched controls were excluded.

This has been further supported by a recent study notable due to its large number of patients across multiple institutions and for its retrospective cohort design. Arasu et al (87) demonstrated a higher cancer risk with each higher level of BPE (hazard ratios: 1.8 for mild BPE, 2.42 for moderate BPE, and 3.41 for marked

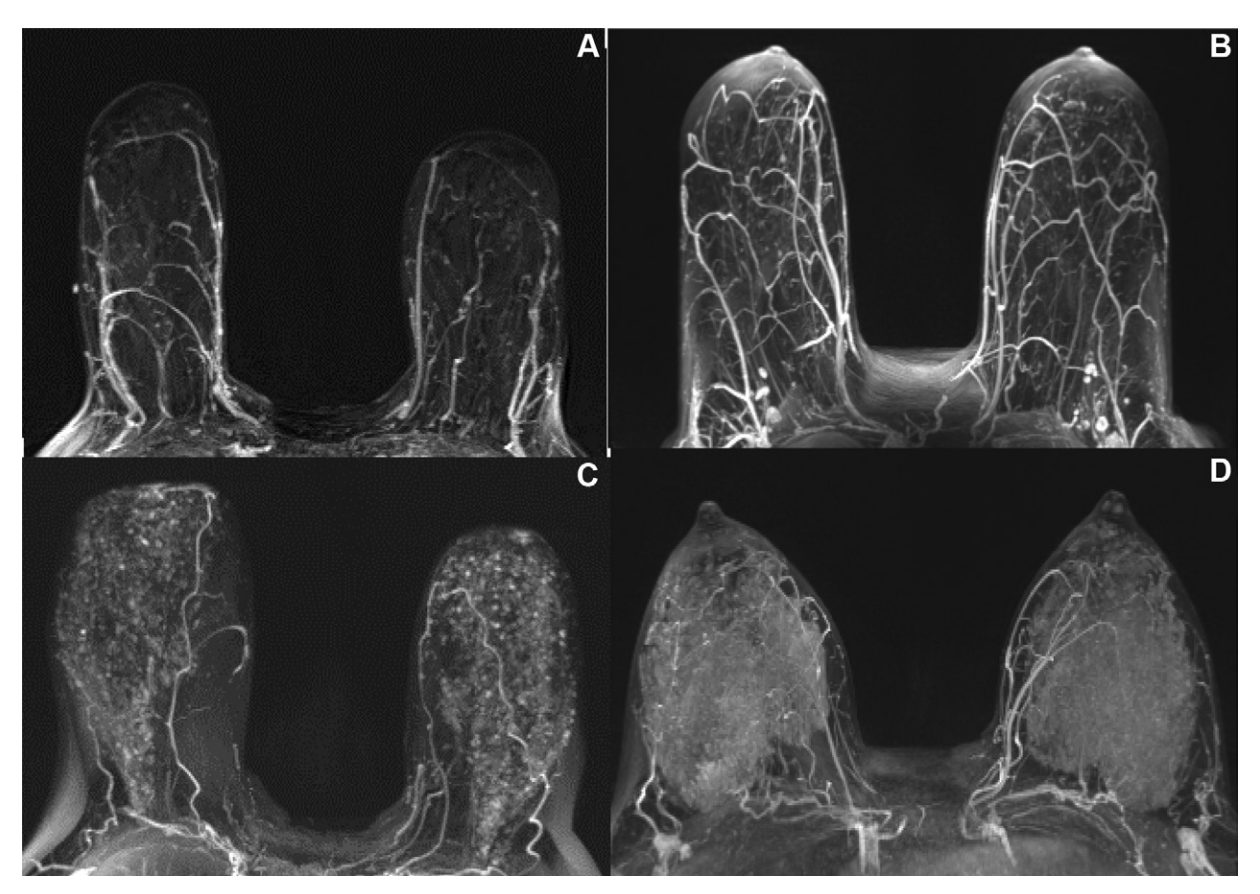


Figure 10: Qualitative background parenchymal enhancement (BPE) assessment according to the Breast Imaging Reporting and Data System lexicon. Axial, subtracted, postcontrast, maximum intensity projection breast MRI scans show (A) minimal, (B) mild, (C) moderate, and (D) marked BPE in four patients.

BPE). Additionally, they found BPE strongly predicted a future diagnosis of invasive breast cancer rather than ductal carcinoma in situ, supporting the use of BPE as a relevant imaging marker for breast cancer.

#### BPE in Women with Elevated Risk

Most of the studies yielding an association of BPE with breast cancer risk have been performed in a cross section of women at high risk as this is the population for whom screening MRI is indicated (79) (Fig 11). Studies of women with a personal history of breast cancer showed that in this group of women at high risk, BPE is associated with a higher risk of developing a second breast cancer or interval breast cancer (92,93). The significance of BPE as a risk factor in women with genetic alterations may be different than for other women at high risk. Studies have shown that BRCA1 and BRCA2 variant carriers have lower BPE and less fibroglandular tissue than age-matched controls (94). BPE has been shown to be reduced in BRCA1 and BRCA2 variant carriers after risk-reducing salpingo-oophorectomy, suggesting that the decreased BPE reflects the hormonal changes from risk-reducing salpingo-oophorectomy, which in turn decreases breast cancer risk (95). A higher BPE level prior to risk-reducing salpingo-oophorectomy has been associated with future breast cancer (85,96). However, the literature shows mixed results regarding a change in BPE after risk-reducing salpingo-oophorectomy. DeLeo et al (85) found that BRCA1 and

BRCA2 variant carriers who did not have a reduction in BPE after risk-reducing salpingo-oophorectomy had a higher risk of subsequent breast cancer, while Bermot et al (96) conversely found that a greater reduction in BPE after risk-reducing salpingo-oophorectomy was associated with a higher risk of breast cancer. Findings of both groups suggest that BPE is a phenotypic imaging marker to identify BRCA1 and BRCA2 variant carriers who may be at risk for developing breast cancer despite risk-reducing salpingo-oophorectomy (85,96). However, whether the initial high BPE level or the change in BPE after risk-reducing salpingo-oophorectomy is the more contributory BPE measure predicting a higher risk of breast cancer remains to be confirmed.

#### BPE in Women with Average Risk

The few studies evaluating women at average risk show mixed results. The meta-analysis by Thompson et al (90) showed no significant association between BPE and breast cancer in the population at average risk (Fig 12). A single-institution study of 540 women at average risk who received breast MRI for suspicious or equivocal findings at conventional imaging or clinical suspicion of cancer also showed no association between BPE and breast cancer risk (97). However, the multi-institution study by Arasu et al (87) showed that women at average lifetime risk (estimated by a 5-year Breast Cancer Surveillance Consortium risk score of <1.67%) with at least mild BPE had an elevated breast cancer risk (a 2.9 times hazard ratio) than those with minimal BPE. Paradoxically,

Study and Year	Study Design	Samples	Indication for MRI	BPE Threshold	Findings
King et al (2011) (78)	Retrospective matched 1:2 case control	39 cancers, 116 controls	High-risk screening	At least moderate BPE	Higher BPE associated with cancer (OR, 6.7)
DeLeo et al (2015) (85)	Retrospective cohort	55 patients, 9 cancers	BRCA1/BRCA2 carriers treated with RRSO	Mean BPE before and after RRSO	Higher BPE before and after RRSO associated with cancer
Albert et al (2015) (114)	Retrospective unmatched case-control	403 cancers, 72 controls	Extent of disease and high-risk screening	BI-RADS categories of BPE	Lower BPE associated with breast cancer in postmenopausal women
Cho et al (2015) (115)	Retrospective unmatched case- control	38 cancers, 39 controls	High-risk screening	BPE percentage	Higher mean BPE associated with cance
Dontchos et al (2015) (116)	Retrospective matched 1:1 case-control	23 cancers, 23 controls	High-risk screening	At least mild BPE	Higher BPE associated with cancer (OR, 9.0
Telegrafo et al (2016) (117)	Retrospective cross- sectional	162 cancers, 224 controls	High-risk screening, problem solving, and extent of disease	At least moderate BPE	Higher BPE associated with cancer
Wu et al (2015) (86)	Retrospective cohort	6 cancers, 44 controls	BRCA1/BRCA2 variant carriers who underwent RRSO	BPE above a threshold	Higher BPE after RRSC associated with cance
Bennani-Baiti et al (2016) (97)	Retrospective cross- sectional	353 cancers, 187 benign	Problem solving and extent of disease	At least moderate BPE	No association of BPE with cancer
Melsaether et al (2017) (118)	Retrospective matched 1:1 case-control	116 cancers, 116 controls	Known breast cancer and age- matched controls with screening or diagnostic MRI	BPE at multiple time points	No association of BPE with cancer
Melsaether et al (2017) (118)	Retrospective cohort	9 cancers, 83 negative	High-risk screening or diagnostic MRI	At least mild BPE	Higher BPE associated with breast cancer only for one reader (OR, 7.67)
Choi et al (2016) (119)	Retrospective cohort	602 patients, 83 cancers	Personal history of breast cancer	At least moderate BPE	Higher BPE associated with recurrence, including early and late recurrence (HR, 2.08)
Hu et al (2017) (88)	Retrospective matched 1:1 case-control	101 cancers, 101 negative, 101 benign	Not reported	Automated ratio of BPE to FGT	Higher BPE associated with cancer (OR, 2.6 in premenopausal women; OR, 2.8 in postmenopausal women)
Wu et al (2017) (120)	Retrospective matched 1:1 case-control	51 cancers, 51 controls	Controls with biopsy- proven benign lesions	Automated BPE percentage	Higher BPE associated with cancer (OR, 3.5)
Lam et al (2019) (121)	Retrospective matched 1:1 case control	23 cancers, 23 controls	High-risk screening	Percent enhancement for each voxel within FGT	Higher BPE associated with cancer
Bermot et al (2018) (96)	Retrospective cohort	146 patients, 26 cancers	BRCA1/BRCA2 variant carriers and women at high risk who underwent RRSO	At least mild BPE at pre-RRSO examination, change in BPE before and after RRSO	Higher BPE at pre- RRSO examination associated with cance (HR, 3.9); reduced BPE at post-RRSO MRI associated with cancer (HR, 2.2)

Study and Year	Study Design	Samples	Indication for MRI	BPE Threshold	Findings
Grimm et al (2019) (122)	Retrospective matched 1:2 case-control	61 cancers, 122 controls	High-risk screening	At least mild BPE at first time point	Higher BPE associated with cancer (OR, 2.5)
Arasu et al (2019) (87)	Retrospective cohort, multicenter study	4247 patients, 176 cancers	High-risk screening and diagnostic	At least mild BPE at first time point	Higher BPE associated with cancer (HR: 1.8 for mild BPE, 2.42 for moderate BPE, and 3.41 for marked BPE) and greater for invasive cancers than DCIS
Sippo et al (2019) (123)	Retrospective cohort	73 cancers, 4613 examinations without cancer	High-risk screening	At least moderate BPE	Higher BPE associated with breast cancer (OR, 2.14 when compared with minimal and/or mild BPE)
Vreemann et al (2019) (124)	Retrospective cohort	60 cancers, 1473 negative	High-risk screening	Automated BPE percentages	No association of BPE with cancer
Saha et al (2019) (105)	Retrospective matched 1:2 case-control	46 cancers, 87 controls	High-risk screening	Automated BPE features, at least mild BPE	Higher BPE associated with breast cancer (OR, 2.44 for readers; OR, 4.21 for automated features)
Watt et al (2020) (125)	Retrospective matched 1:1 case-control, multicenter study	835 cancers, 963 controls	Not reported	At least mild and at least moderate BPE	At least moderate BPE associated with breast cancer (OR,1.49) in premenopausal women; at least mild BPE associated with breast cancer (OR, 1.45) in postmenopausal women
Niell et al (2021) (103)	Retrospective matched 1:4 case-control	19 cancers, 76 controls	High-risk screening	At least mild BPE	Higher BPE associated with breast cancer (OR, 3.0)
Kim et al (2021) (92)	Retrospective cohort	examinations in 2809 women, 10 interval cancers	Personal history of breast cancer	At least moderate BPE	Higher BPE associated with interval cancer (OR, 14.5)
Lee et al (2022) (93)	Retrospective cohort	2668 women, 109 cancers	Personal history of breast cancer	At least mild BPE	Higher BPE associated with future second breast cancer (HR, 2.1)

this same study found that although higher BPE was associated with a higher risk of breast cancer in women with a history of a first-degree relative with breast cancer, this association did not hold in women without a family history. Thompson et al (90) have suggested that BPE may indicate a healthy breast tissue phenomenon in women at average risk, while breast tissue in high-risk patients is biologically different than normal breast tissue. Given the grow-

ing acceptance of abbreviated MRI to expand MRI screening for women at average and intermediate risk, the significance of BPE in these groups requires additional study.

#### Future Directions in MRI

There is wide variability in the MRI sequences and quantitative methods used for BPE assessment (98). In addition, there

is significant interest in providing supplemental screening to women at otherwise average risk but who have dense breasts by using abbreviated, or "fast," breast MRI where only limited post-contrast imaging is performed to improve cost-effectiveness and maintain sensitivity of cancer detection (99–102). In the future, risk prediction models will likely incorporate BPE as a quantitative imaging marker to provide more refined individualized results (103). The change in BPE after risk-reducing interventions, such as bilateral salpingo-oophorectomy or tamoxifen use, may also be incorporated into models quantifying the degree of risk reduction to personalize a patient's preventive strategy.

Development of generalizable risk prediction models will first require standardization of quantitative BPE. Deep learning models will likely become valuable tools in providing automated, accurate, and reproducible BPE assessments (104,105). Deep learning models may also be trained on contrast-enhanced MRI scans and incorporate all the information present in the image, beyond BPE information alone, to refine risk prediction (106).

BPE is also being studied as a prognostic and predictive imaging marker in women diagnosed with breast cancer because BPE has been associated with tumor type (107), response to neoadjuvant therapy (108), and recurrence-free survival (109).

# **Future Directions and Clinical Implementation**

Beyond the use of mammographic density alone to identify women at high risk for breast cancer, the goal of the imaging markers described in this article is to develop personalized screening strategies for breast imaging. As of November 2022, there continue

> to be hurdles to widespread implementation of these imaging markers, such as image-based deep learning (49,50), despite promising results over traditional risk models. These hurdles include the need for validation and prospective trials across diverse populations and sites (110,111), as well as the need for standardization of risk assessment and reporting.

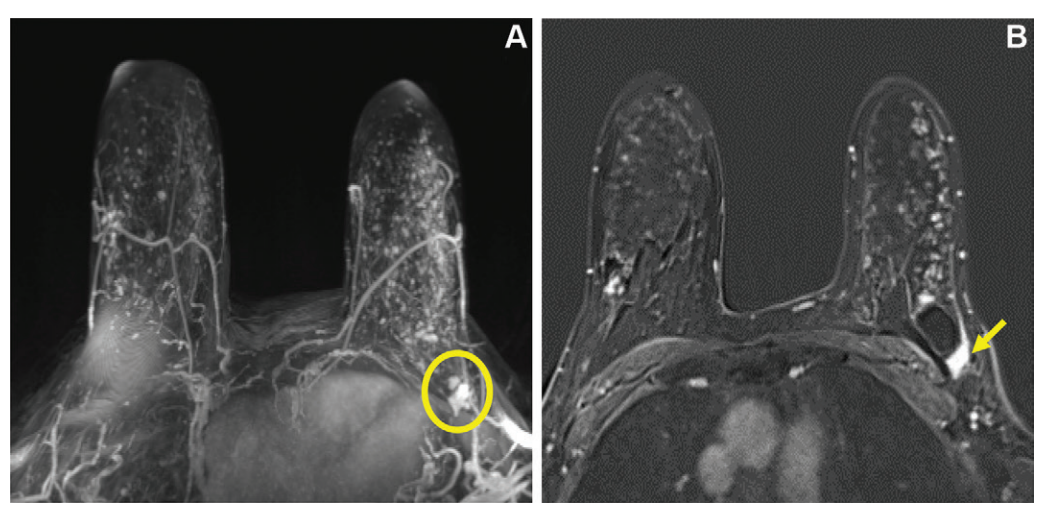


Figure 11: Images in a 46-year-old woman at high risk for breast cancer due to strong family history (calculated lifetime risk of 33%). Screening MRI demonstrated extreme fibroglandular tissue. (A) Axial, subtracted, postcontrast maximum intensity projection MRI scan shows moderate background parenchymal enhancement (BPE) and a mass in the left axillary tail (circle). (B) Postcontrast, T1-weighted subtracted axial MRI scan with the section centered at the level of the left breast mass shows the enhancing irregular mass (arrow) that was subsequently biopsied yielding moderately differentiated carcinoma with mixed ductal and lobular features. A higher BPE level has been associated with risk of breast cancer in women at high risk.

# Conclusion

Herein, we describe a range of imaging markers associated with breast cancer risk, with the ultimate goal of enabling personalized screening strategies.

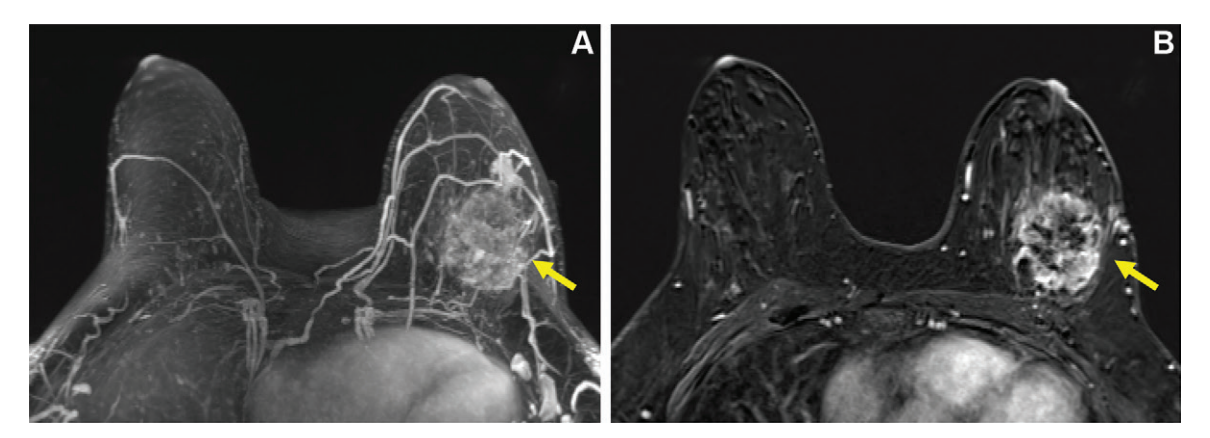


Figure 12: Images in a 34-year-old woman without family history of breast cancer with newly diagnosed left breast cancer manifesting as a palpable lump. MRI performed for extent of disease demonstrates heterogeneous fibroglandular tissue. (A) Axial, subtracted, postcontrast maximum intensity projection MRI scan shows minimal background parenchymal enhancement (BPE) and a mass in the left lateral breast (arrow). (B) Postcontrast, T1-weighted subtracted axial MRI scan with the section centered at the level of the left breast mass shows the enhancing irregular mass (arrow) that was subsequently biopsied yielding poorly differentiated invasive ductal carcinoma. Studies show mixed results regarding the association between BPE and breast cancer in patients at average risk (ie, without family history of breast cancer or known deleterious genetic alteration).

Disclosures of conflicts of interest: R.J.A. Grants from the Breast Cancer Alliance, Burroughs Wellcome Fund, U.S. Department of Defense Breast Cancer Research Program, and National Institutes of Health (NIH); patents planned, issued, or pending. S.H.L. No relevant relationships. B.R. No relevant relationships. L.M. Editor, Radiology; grants from Siemens Healthcare, Gordon and Betty Moore Foundation, Mary Kay Foundation, and Google; personal fees, Lunit Insight, iCAD advisory board, Guerbet; meeting and travel expenses, British Society of Breast Radiology and European Society of Breast Imaging. E.F.C. Grants or contracts from iCAD, Hologic, and OM1; payment or honoraria from MedScape and Aunt Minnie; lecture travel support from the RSNA for European Congress of Radiology 2022; advisory board, iCAD and Hologic current board member, Society of Breast Imaging. D.K. Grants from NIH; institutional research agreement with iCAD; patents planned, issued, or pending. W.K.M. Institutional research grant from Bayer.

#### References

- Vachon CM, van Gils CH, Sellers TA, et al. Mammographic density, breast cancer risk and risk prediction. Breast Cancer Res 2007;9(6):217.
- Holland K, van Gils CH, Mann RM, Karssemeijer N. Quantification of masking risk in screening mammography with volumetric breast density maps. Breast Cancer Res Treat 2017;162(3):541–548.
- Sherratt MJ, McConnell JC, Streuli CH. Raised mammographic density: causative mechanisms and biological consequences. Breast Cancer Res 2016;18(1):45.
- Johns PC, Yaffe MJ. X-ray characterisation of normal and neoplastic breast tissues. Phys Med Biol 1987;32(6):675–695.
- Checka CM, Chun JE, Schnabel FR, Lee J, Toth H. The relationship of mammographic density and age: implications for breast cancer screening. AJR Am J Roentgenol 2012;198(3):W292–W295.
- Boyd NF, Martin LJ, Sun L, et al. Body size, mammographic density, and breast cancer risk. Cancer Epidemiol Biomarkers Prev 2006;15(11):2086– 2092.
- Greendale GA, Reboussin BA, Slone S, Wasilauskas C, Pike MC, Ursin G. Postmenopausal hormone therapy and change in mammographic density. J Natl Cancer Inst 2003;95(1):30–37.
- Cuzick J, Warwick J, Pinney E, Warren RML, Duffy SW. Tamoxifen and breast density in women at increased risk of breast cancer. J Natl Cancer Inst 2004;96(8):621–628.
- Grove JS, Goodman MJ, Gilbert FI Jr, Mi MP. Factors associated with mammographic pattern. Br J Radiol 1985;58(685):21–25.
- Sprague BL, Gangnon RE, Burt V, et al. Prevalence of mammographically dense breasts in the United States. J Natl Cancer Inst 2014;106(10):dju255.
- Dehkordy SF, Carlos RC. Dense Breast Legislation in the United States: State
  of the States. J Am Coll Radiol 2016;13(11S):R53–R57. [Published correction appears in J Am Coll Radiol 2018;15(10):1522.]
- Berg WA, Blume JD, Cormack JB, et al; ACRIN 6666 Investigators. Combined screening with ultrasound and mammography vs mammography alone in women at elevated risk of breast cancer. JAMA 2008;299(18): 2151–2163.
- 13. Bakker MF, de Lange SV, Pijnappel RM, et al; DENSE Trial Study Group. Supplemental MRI Screening for Women with Extremely Dense Breast Tissue. N Engl J Med 2019;381(22):2091–2102.
- Karimi Z, Phillips J, Slanetz P, et al. Factors Associated With Background Parenchymal Enhancement on Contrast-Enhanced Mammography. AJR Am J Roentgenol 2021;216(2):340–348.
- Sorin V, Yagil Y, Shalmon A, et al. Background Parenchymal Enhancement at Contrast-Enhanced Spectral Mammography (CESM) as a Breast Cancer Risk Factor. Acad Radiol 2020;27(9):1234–1240.
- Hruska CB, Geske JR, Conners AL, et al. Background Parenchymal Uptake on Molecular Breast Imaging and Breast Cancer Risk: A Cohort Study. AJR Am J Roentgenol 2021;216(5):1193–1204.
- Wolfe JN. Breast patterns as an index of risk for developing breast cancer. AJR Am J Roentgenol 1976;126(6):1130–1137.
- Gram IT, Funkhouser E, Tabár L. The Tabár classification of mammographic parenchymal patterns. Eur J Radiol 1997;24(2):131–136.
- Boyd NF, Jensen HM, Cooke G, Han HL. Relationship between mammographic and histological risk factors for breast cancer. J Natl Cancer Inst 1992;84(15):1170–1179.
- D'Orsi CJ, Bassett LW, Berg WA, Feig SA, Jackson V, Kopans D. Breast Imaging Reporting and Data System: ACR BI-RADS Mammography. American College of Radiology; 2003.
- Sickles EA, D'Orsi CJ, Bassett LW, et al. ACR BI-RADS Mammography. In: ACR BI-RADS Atlas, Breast Imaging Reporting and Data System. American College of Radiology; 2013.
- 22. Sprague BL, Conant EF, Onega T, et al; PROSPR Consortium. Variation in Mammographic Breast Density Assessments Among Radiologists

- in Clinical Practice: A Multicenter Observational Study. Ann Intern Med 2016;165(7):457–464.
- Gastounioti A, Desai S, Ahluwalia VS, Conant EF, Kontos D. Artificial intelligence in mammographic phenotyping of breast cancer risk: a narrative review. Breast Cancer Res 2022;24(1):14.
- Lehman CD, Yala A, Schuster T, et al. Mammographic Breast Density Assessment Using Deep Learning: Clinical Implementation. Radiology 2019;290(1):52–58.
- Kallenberg M, Petersen K, Nielsen M, et al. Unsupervised Deep Learning Applied to Breast Density Segmentation and Mammographic Risk Scoring. IEEE Trans Med Imaging 2016;35(5):1322–1331.
- Li S, Wei J, Chan HP, et al. Computer-aided assessment of breast density: comparison of supervised deep learning and feature-based statistical learning. Phys Med Biol 2018;63(2):025005.
- Haji Maghsoudi O, Gastounioti A, Scott C, et al. Deep-LIBRA: An artificial-intelligence method for robust quantification of breast density with independent validation in breast cancer risk assessment. Med Image Anal 2021;73:102138.
- Lamb LR, Lehman CD, Gastounioti A, Conant EF, Bahl M. Artificial Intelligence (AI) for Screening Mammography, From the AJR Special Series on AI Applications. AJR Am J Roentgenol 2022;219(3):369–380.
- Li J, Szekely L, Eriksson L, et al. High-throughput mammographic-density measurement: a tool for risk prediction of breast cancer. Breast Cancer Res 2012;14(4):R114.
- Nickson C, Arzhaeva Y, Aitken Z, et al. AutoDensity: an automated method to measure mammographic breast density that predicts breast cancer risk and screening outcomes. Breast Cancer Res 2013;15(5):R80.
- Mandrekar JN. Receiver operating characteristic curve in diagnostic test assessment. J Thorac Oncol 2010;5(9):1315–1316.
- Brandt KR, Scott CG, Ma L, et al. Comparison of Clinical and Automated Breast Density Measurements: Implications for Risk Prediction and Supplemental Screening. Radiology 2016;279(3):710–719.
- Warwick J, Birke H, Stone J, et al. Mammographic breast density refines Tyrer-Cuzick estimates of breast cancer risk in high-risk women: findings from the placebo arm of the International Breast Cancer Intervention Study I. Breast Cancer Res 2014;16(5):451.
- 34. Keller BM, Chen J, Daye D, Conant EF, Kontos D. Preliminary evaluation of the publicly available Laboratory for Breast Radiodensity Assessment (LIBRA) software tool: comparison of fully automated area and volumetric density measures in a case-control study with digital mammography. Breast Cancer Res 2015;17(1):117.
- Brentnall AR, Harkness EF, Astley SM, et al. Mammographic density adds accuracy to both the Tyrer-Cuzick and Gail breast cancer risk models in a prospective UK screening cohort. Breast Cancer Res 2015;17(1):147.
- Brentnall AR, Cohn WF, Knaus WA, Yaffe MJ, Cuzick J, Harvey JA. A Case-Control Study to Add Volumetric or Clinical Mammographic Density into the Tyrer-Cuzick Breast Cancer Risk Model. J Breast Imaging 2019;1(2):99– 106.
- Gastounioti A, Conant EF, Kontos D. Beyond breast density: a review on the advancing role of parenchymal texture analysis in breast cancer risk assessment. Breast Cancer Res 2016;18(1):91.
- 38. Zheng Y, Keller BM, Ray S, et al. Parenchymal texture analysis in digital mammography: A fully automated pipeline for breast cancer risk assessment. Med Phys 2015;42(7):4149–4160.
- Kontos D, Winham SJ, Oustimov A, et al. Radiomic Phenotypes of Mammographic Parenchymal Complexity: Toward Augmenting Breast Density in Breast Cancer Risk Assessment. Radiology 2019;290(1):41–49.
- Manduca A, Carston MJ, Heine JJ, et al. Texture features from mammographic images and risk of breast cancer. Cancer Epidemiol Biomarkers Prev 2009;18(3):837–845.
- Wei J, Chan HP, Wu YT, et al. Association of computerized mammographic parenchymal pattern measure with breast cancer risk: a pilot case-control study. Radiology 2011;260(1):42–49.
- Sun W, Tseng TLB, Qian W, et al. Using multiscale texture and density features for near-term breast cancer risk analysis. Med Phys 2015;42(6):2853

  2862.
- Huo Z, Giger ML, Olopade OI, et al. Computerized analysis of digitized mammograms of BRCA1 and BRCA2 gene mutation carriers. Radiology 2002;225(2):519–526.
- Gierach GL, Li H, Loud JT, et al. Relationships between computer-extracted mammographic texture pattern features and BRCA1/2 mutation status: a cross-sectional study. Breast Cancer Res 2014;16(4):424.
- Li H, Giger ML, Lan L, Janardanan J, Sennett CA. Comparative analysis
  of image-based phenotypes of mammographic density and parenchymal patterns in distinguishing between BRCA1/2 cases, unilateral cancer cases, and
  controls. J Med Imaging (Bellingham) 2014;1(3):031009.

- Arefan D, Mohamed AA, Berg WA, Zuley ML, Sumkin JH, Wu S. Deep learning modeling using normal mammograms for predicting breast cancer risk. Med Phys 2020;47(1):110–118.
- Dembrower K, Liu Y, Azizpour H, et al. Comparison of a Deep Learning Risk Score and Standard Mammographic Density Score for Breast Cancer Risk Prediction. Radiology 2020;294(2):265–272.
- Ha R, Chang P, Karcich J, et al. Convolutional Neural Network Based Breast Cancer Risk Stratification Using a Mammographic Dataset. Acad Radiol 2019;26(4):544–549.
- Yala A, Lehman C, Schuster T, Portnoi T, Barzilay R. A Deep Learning Mammography-based Model for Improved Breast Cancer Risk Prediction. Radiology 2019;292(1):60–66.
- 50. Yala A, Mikhael PG, Strand F, et al. Toward robust mammography-based models for breast cancer risk. Sci Transl Med 2021;13(578):eaba4373.
- Sechopoulos I. A review of breast tomosynthesis. Part I. The image acquisition process. Med Phys 2013;40(1):014301.
- Sechopoulos I. A review of breast tomosynthesis. Part II. Image reconstruction, processing and analysis, and advanced applications. Med Phys 2013;40(1):014302.
- Ratanaprasatporn L, Chikarmane SA, Giess CS. Strengths and Weaknesses of Synthetic Mammography in Screening. RadioGraphics 2017;37(7):1913– 1927.
- 54. Alabousi M, Wadera A, Kashif Al-Ghita M, et al. Performance of Digital Breast Tomosynthesis, Synthetic Mammography, and Digital Mammography in Breast Cancer Screening: A Systematic Review and Meta-Analysis. J Natl Cancer Inst 2021;113(6):680–690.
- Tice JA, Gard CC, Miglioretti DL, et al. Comparing Mammographic Density Assessed by Digital Breast Tomosynthesis or Digital Mammography: The Breast Cancer Surveillance Consortium. Radiology 2022;302(2):286–292.
- Haider I, Morgan M, McGow A, et al. Comparison of Breast Density Between Synthesized Versus Standard Digital Mammography. J Am Coll Radiol 2018;15(10):1430–1436.
- Gastounioti A, McCarthy AM, Pantalone L, Synnestvedt M, Kontos D, Conant EF. Effect of Mammographic Screening Modality on Breast Density Assessment: Digital Mammography versus Digital Breast Tomosynthesis. Radiology 2019;291(2):320–327.
- Aujero MP, Gavenonis SC, Benjamin R, Zhang Z, Holt JS. Clinical Performance of Synthesized Two-dimensional Mammography Combined with Tomosynthesis in a Large Screening Population. Radiology 2017;283(1): 70–76.
- Zuckerman SP, Conant EF, Keller BM, et al. Implementation of Synthesized Two-dimensional Mammography in a Population-based Digital Breast Tomosynthesis Screening Program. Radiology 2016;281(3):730–736.
- Lotter W, Diab AR, Haslam B, et al. Robust breast cancer detection in mammography and digital breast tomosynthesis using an annotation-efficient deep learning approach. Nat Med 2021;27(2):244–249.
- Eriksson M, Destounis S, Czene K, et al. A risk model for digital breast tomosynthesis to predict breast cancer and guide clinical care. Sci Transl Med 2022;14(644):eabn3971.
- Eriksson M, Czene K, Strand F, et al. Identification of Women at High Risk of Breast Cancer Who Need Supplemental Screening. Radiology 2020;297(2):327–333.
- Mendelson EB, Böhm-Vélez M, Berg WA, et al. ACR BI-RADS Ultrasound. In: ACR BI-RADS Atlas, Breast Imaging Reporting and Data System. American College of Radiology; 2013.
- 64. Blend R, Rideout DF, Kaizer L, Shannon P, Tudor-Roberts B, Boyd NF. Parenchymal patterns of the breast defined by real time ultrasound. Eur J Cancer Prev 1995;4(4):293–298.
- Rubin CS, Kurtz AB, Goldberg BB, Feig S, Cole-Beuglet C. Ultrasonic mammographic parenchymal patterns: a preliminary report. Radiology 1979;130(2):515–517.
- Glide-Hurst CK, Duric N, Littrup P. Volumetric breast density evaluation from ultrasound tomography images. Medical physics 2008;35(9):3988– 3997.
- Kim WH, Moon WK, Kim SJ, et al. Ultrasonographic assessment of breast density. Breast Cancer Res Treat 2013;138(3):851–859.
- Izumori A, Horii R, Akiyama F, Iwase T. Proposal of a novel method for observing the breast by high-resolution ultrasound imaging: understanding the normal breast structure and its application in an observational method for detecting deviations. Breast Cancer 2013;20(1):83–91.
- Hou XY, Niu HY, Huang XL, Gao Y. Correlation of Breast Ultrasound Classifications with Breast Cancer in Chinese Women. Ultrasound Med Biol 2016;42(11):2616–2621.
- Lee SH, Ryu HS, Jang MJ, et al. Glandular Tissue Component and Breast Cancer Risk in Mammographically Dense Breasts at Screening Breast US. Radiology 2021;301(1):57–65.

- Kim SH, Kim HH, Moon WK. Automated Breast Ultrasound Screening for Dense Breasts. Korean J Radiol 2020;21(1):15–24.
- Chang RF, Hou YL, Lo CM, et al. Quantitative analysis of breast echotexture patterns in automated breast ultrasound images. Med Phys 2015;42(8):4566– 4578.
- McKian KP, Reynolds CA, Visscher DW, et al. Novel breast tissue feature strongly associated with risk of breast cancer. J Clin Oncol 2009;27(35):5893– 5898.
- Ghosh K, Hartmann LC, Reynolds C, et al. Association between mammographic density and age-related lobular involution of the breast. J Clin Oncol 2010;28(13):2207–2212.
- Bao Z, Zhao Y, Chen S, et al. Evidence and assessment of parenchymal patterns of ultrasonography for breast cancer detection among Chinese women: a cross-sectional study. BMC Med Imaging 2021;21(1):152.
- Sung JS, Stamler S, Brooks J, et al. Breast Cancers Detected at Screening MR Imaging and Mammography in Patients at High Risk: Method of Detection Reflects Tumor Histopathologic Results. Radiology 2016;280(3): 716–722.
- Morris EA, Comstock CE, Lee CH, et al. ACR BI-RADS Magnetic Resonance Imaging. In: ACR BI-RADS Atlas, Breast Imaging Reporting and Data System. American College of Radiology; 2013.
- King V, Brooks JD, Bernstein JL, Reiner AS, Pike MC, Morris EA. Background parenchymal enhancement at breast MR imaging and breast cancer risk. Radiology 2011;260(1):50–60.
- Liao GJ, Henze Bancroft LC, Strigel RM, et al. Background parenchymal enhancement on breast MRI: A comprehensive review. J Magn Reson Imaging 2020;51(1):43–61.
- Jung Y, Jeong SK, Kang DK, Moon Y, Kim TH. Quantitative analysis of background parenchymal enhancement in whole breast on MRI: Influence of menstrual cycle and comparison with a qualitative analysis. Eur J Radiol 2018;103:84

  –89.
- 81. King V, Gu Y, Kaplan JB, Brooks JD, Pike MC, Morris EA. Impact of menopausal status on background parenchymal enhancement and fibroglandular tissue on breast MRI. Eur Radiol 2012;22(12):2641–2647.
- King V, Goldfarb SB, Brooks JD, et al. Effect of aromatase inhibitors on background parenchymal enhancement and amount of fibroglandular tissue at breast MR imaging. Radiology 2012;264(3):670–678.
- King V, Kaplan J, Pike MC, et al. Impact of tamoxifen on amount of fibroglandular tissue, background parenchymal enhancement, and cysts on breast magnetic resonance imaging. Breast J 2012;18(6):527–534.
- Kuhl CK. Predict, Then Act: Moving Toward Tailored Prevention. J Clin Oncol 2019;37(12):943–945.
- DeLeo MJ 3rd, Domchek SM, Kontos D, Conant E, Chen J, Weinstein S. Breast MRI fibroglandular volume and parenchymal enhancement in BRCA1 and BRCA2 mutation carriers before and immediately after risk-reducing salpingo-oophorectomy. AJR Am J Roentgenol 2015;204(3):669–673.
- 86. Wu S, Weinstein SP, DeLeo MJ 3rd, et al. Quantitative assessment of background parenchymal enhancement in breast MRI predicts response to risk-reducing salpingo-oophorectomy: preliminary evaluation in a cohort of BRCA1/2 mutation carriers. Breast Cancer Res 2015;17(1):67. [Published correction appears in Breast Cancer Res 2015;17:144.]
- Arasu VA, Miglioretti DL, Sprague BL, et al. Population-Based Assessment of the Association Between Magnetic Resonance Imaging Background Parenchymal Enhancement and Future Primary Breast Cancer Risk. J Clin Oncol 2019;37(12):954–963.
- Hu X, Jiang L, Li Q, Gu Y. Quantitative assessment of background parenchymal enhancement in breast magnetic resonance images predicts the risk of breast cancer. Oncotarget 2017;8(6):10620–10627.
- Sung JS, Corben AD, Brooks JD, et al. Histopathologic characteristics of background parenchymal enhancement (BPE) on breast MRI. Breast Cancer Res Treat 2018;172(2):487–496.
- Thompson CM, Mallawaarachchi I, Dwivedi DK, et al. The Association of Background Parenchymal Enhancement at Breast MRI with Breast Cancer: A Systematic Review and Meta-Analysis. Radiology 2019;292(3):552–561.
- Hu N, Zhao J, Li Y, et al. Breast cancer and background parenchymal enhancement at breast magnetic resonance imaging: a meta-analysis. BMC Med Imaging 2021;21(1):32.
- Kim GR, Cho N, Kim SY, Han W, Moon WK. Interval Cancers after Negative Supplemental Screening Breast MRI Results in Women with a Personal History of Breast Cancer. Radiology 2021;300(2):314–323.
- Lee SH, Jang MJ, Yoen H, et al. Background Parenchymal Enhancement at Postoperative Surveillance Breast MRI: Association with Future Second Breast Cancer Risk. Radiology 2022. 10.1148/radiol.220440. Published online August 30, 2022.
- 94. Grubstein A, Rapson Y, Benzaquen O, et al. Comparison of background parenchymal enhancement and fibroglandular density at breast magnetic reso-

- nance imaging between BRCA gene mutation carriers and non-carriers. Clin Imaging 2018;51:347–351.
- Price ER, Brooks JD, Watson EJ, Brennan SB, Comen EA, Morris EA. The impact of bilateral salpingo-oophorectomy on breast MRI background parenchymal enhancement and fibroglandular tissue. Eur Radiol 2014;24(1):162– 168.
- Bermot C, Saint-Martin C, Malhaire C, et al. Background parenchymal enhancement and fibroglandular tissue on breast MRI in women with high genetic risk: Are changes before and after risk-reducing salpingo-oophorectomy associated with breast cancer risk? Eur J Radiol 2018;109:171–177.
- 97. Bennani-Baiti B, Dietzel M, Baltzer PA. MRI Background Parenchymal Enhancement Is Not Associated with Breast Cancer. PLoS One 2016;11 (7):e0158573 [Published correction appears in PLoS One 2016;11(9):e0162936.].
- 98. Bignotti B, Signori A, Valdora F, et al. Evaluation of background parenchymal enhancement on breast MRI: a systematic review. Br J Radiol 2017;90(1070):20160542.
- Kuhl C, Weigel S, Schrading S, et al. Prospective multicenter cohort study to refine management recommendations for women at elevated familial risk of breast cancer: the EVA trial. J Clin Oncol 2010;28(9):1450–1457.
- 100. Kuhl CK, Schrading S, Strobel K, Schild HH, Hilgers RD, Bieling HB. Abbreviated breast magnetic resonance imaging (MRI): first postcontrast subtracted images and maximum-intensity projection-a novel approach to breast cancer screening with MRI. J Clin Oncol 2014;32(22):2304–2310.
- 101. Weinstein SP, Korhonen K, Cirelli C, et al. Abbreviated Breast Magnetic Resonance Imaging for Supplemental Screening of Women With Dense Breasts and Average Risk. J Clin Oncol 2020;38(33):3874–3882.
- 102. Comstock CE, Gatsonis C, Newstead GM, et al. Comparison of Abbreviated Breast MRI vs Digital Breast Tomosynthesis for Breast Cancer Detection Among Women With Dense Breasts Undergoing Screening. JAMA 2020;323(8):746–756.
- 103. Niell BL, Abdalah M, Stringfield O, et al. Quantitative Measures of Background Parenchymal Enhancement Predict Breast Cancer Risk. AJR Am J Roentgenol 2021;217(1):64–75.
- 104. Eskreis-Winkler S, Sutton EJ, D'Alessio D, et al. Breast MRI Background Parenchymal Enhancement Categorization Using Deep Learning: Outperforming the Radiologist. J Magn Reson Imaging 2022;56(4):1068–1076.
- 105. Saha A, Grimm LJ, Ghate SV, et al. Machine learning-based prediction of future breast cancer using algorithmically measured background parenchymal enhancement on high-risk screening MRI. J Magn Reson Imaging 2019;50(2):456–464.
- 106. Portnoi T, Yala A, Schuster T, et al. Deep Learning Model to Assess Cancer Risk on the Basis of a Breast MR Image Alone. AJR Am J Roentgenol 2019;213(1):227–233.
- 107. Li J, Mo Y, He B, et al. Association between MRI background parenchymal enhancement and lymphovascular invasion and estrogen receptor status in invasive breast cancer. Br J Radiol 2019;92(1103):20190417.
- 108. Onishi N, Li W, Newitt DC, et al. Breast MRI during Neoadjuvant Chemotherapy: Lack of Background Parenchymal Enhancement Suppression and Inferior Treatment Response. Radiology 2021;301(2):295–308.
- 109. Lim Y, Ko ES, Han BK, et al. Background parenchymal enhancement on breast MRI: association with recurrence-free survival in patients with newly diagnosed invasive breast cancer. Breast Cancer Res Treat 2017;163(3):573– 586.

- 110. Yala A, Mikhael PG, Strand F, et al. Multi-Institutional Validation of a Mammography-Based Breast Cancer Risk Model. J Clin Oncol 2022;40(16):1732–1740.
- 111. Eriksson M, Conant EF, Kontos D, Hall P. Risk Assessment in Population-Based Breast Cancer Screening. J Clin Oncol 2022;40(20):2279–2280.
- 112. Berg WA, Blume JD, Cormack JB, Mendelson EB. Operator dependence of physician-performed whole-breast US: lesion detection and characterization. Radiology 2006;241(2):355–365.
- 113. Lee SH, Yi A, Chang JM, Cho N, Moon WK, Kim SY. Background Echotexture on Breast Ultrasound: Impact on Diagnostic Performance of Supplemental Screening in Women with Negative Mammography (SSE01-04). 103rd Scientific Assembly and Annual Meeting, Radiological Society of North America; McCormick Place, Chicago, 2017 (RSNA Conference Abstract). https://rsna2017.rsna.org/program/.
- 114. Albert M, Schnabel F, Chun J, et al. The relationship of breast density in mammography and magnetic resonance imaging in high-risk women and women with breast cancer. Clin Imaging 2015;39(6):987–992.
- 115. Cho GY, Moy L, Kim SG, et al. Comparison of contrast enhancement and diffusion-weighted magnetic resonance imaging in healthy and cancerous breast tissue. Eur J Radiol 2015;84(10):1888–1893.
- 116. Dontchos BN, Rahbar H, Partridge SC, et al. Are Qualitative Assessments of Background Parenchymal Enhancement, Amount of Fibroglandular Tissue on MR Images, and Mammographic Density Associated with Breast Cancer Risk? Radiology 2015;276(2):371–380.
- 117. Telegrafo M, Rella L, Stabile Ianora AA, Angelelli G, Moschetta M. Breast MRI background parenchymal enhancement (BPE) correlates with the risk of breast cancer. Magn Reson Imaging 2016;34(2):173–176.
- 118. Melsaether A, Pujara AC, Elias K, et al. Background parenchymal enhancement over exam time in patients with and without breast cancer. J Magn Reson Imaging 2017;45(1):74–83.
- 119. Choi EJ, Choi H, Choi SA, Youk JH. Dynamic contrast-enhanced breast magnetic resonance imaging for the prediction of early and late recurrences in breast cancer. Medicine (Baltimore) 2016;95(48):e5330.
- 120. Wu S, Zuley ML, Berg WA, et al. DCE-MRI Background Parenchymal Enhancement Quantified from an Early versus Delayed Post-contrast Sequence: Association with Breast Cancer Presence. Sci Rep 2017;7(1):2115.
- 121.Lam DL, Hippe DS, Kitsch AE, Partridge SC, Rahbar H. Assessment of Quantitative Magnetic Resonance Imaging Background Parenchymal Enhancement Parameters to Improve Determination of Individual Breast Cancer Risk. J Comput Assist Tomogr 2019;43(1):85–92.
- 122. Grimm LJ, Saha A, Ghate SV, et al. Relationship between Background Parenchymal Enhancement on High-risk Screening MRI and Future Breast Cancer Risk. Acad Radiol 2019;26(1):69–75.
- 123. Sippo DA, Rutledge GM, Burk KS, et al. Effect of Background Parenchymal Enhancement on Cancer Risk Across Different High-Risk Patient Populations Undergoing Screening Breast MRI. AJR Am J Roentgenol 2019;212(6):1412–1418.
- 124. Vreemann S, Dalmis MU, Bult P, et al. Amount of fibroglandular tissue FGT and background parenchymal enhancement BPE in relation to breast cancer risk and false positives in a breast MRI screening program: A retrospective cohort study. Eur Radiol 2019;29(9):4678–4690.
- 125. Watt GP, Sung J, Morris EA, et al. Association of breast cancer with MRI background parenchymal enhancement: the IMAGINE case-control study. Breast Cancer Res 2020;22(1):138.